Raman and SERS spectroscopy of cucurbit[*n*]urils†

Sumeet Mahajan,*[a] Tung-Chun Lee,[b] Frank Biedermann,[b] James T. Hugall,[a] Jeremy J. Baumberg[a] and Oren A. Scherman*[b]

Received 30th March 2010, Accepted 3rd June 2010
DOI: 10.1039/c0cp00071j

Cucurbit[*n*]urils (CB[*n*]) are a family of supramolecular hosts which can provide highly selective recognition based on their size (*n*). In this work we study their Raman spectroscopic signatures both experimentally and by molecular simulation and find systematic trends providing evidence of ring strain effects with size. Furthermore, we present for the first time their surface-enhanced Raman scattering (SERS) spectra utilizing both nanostructured surface and nanoparticle based approaches. Using SERS we can detect CB[*n*] at the ppb level and are able to distinguish between them in mixtures. Our study paves the way for utilization of CB[*n*] in highly sensitive, multiplexed, real time and high throughput molecular recognition assays based on SERS.

1. Introduction

Surface enhanced Raman scattering (SERS) based detection schemes can provide high sensitivity, real time information, multiplexed and high throughput assays. Supramolecular hosts for providing specificity through molecular recognition can prove immensely useful in these applications. Cucurbit[*n*]-urils (CB[*n*]) are a family of supramolecular hosts, which are macrocyclic, rigid and highly symmetric.[1] Their selectivity towards the shape and charge of a wide variety of guests is considerably higher than that of cyclodextrins (CDs), one of the classical macrocyclic supramolecular hosts. The association constants (K_a) of their host–guest complexes are typically several orders of magnitude higher than that of CDs. It can be as high as 3×10^{15} M^{-1}, reported for binding between CB[7] and ferrocene derivatives, which is similar to the well-known avidin–biotin pair.[2]

Although NMR[3–5] and X-ray[6] have been used for structurally characterising CB[*n*]s, they often require prolonged duration, are not necessarily suitable to study systems with fast dynamics and are incompatible with high throughput applications, such as medical screening. Furthermore, CB[*n*] supramolecular systems and their complexes have also been studied by other methods, such as ESI-mass spectrometry,[7] UV-vis and fluorescent spectrometry,[8] none of which provide information concerning bonding and structure of the CB[*n*] systems.

Raman spectroscopy is a vibrational spectroscopic technique which gives 'fingerprint' spectra enabling characterization and identification of molecules similar to infrared (IR) spectroscopy. However, Raman spectroscopy has numerous advantages over IR such as tolerance to water and atmospheric CO_2, negligible requirement of sample preparation, clear spectra (generally free of harmonics and overtones) and observation of low frequency vibrations (< 600 cm^{-1}). Nevertheless, its utilization as an aid to synthetic chemists has been rather restricted. This has been primarily due to its comparative weakness in intensity to IR, which is a direct absorption process, while Raman (being an inelastic scattering process) is inherently less efficient. As a consequence of the technological advancements over the past few decades in high power lasers, optics and detectors, it is now possible to acquire Raman spectra as easily as IR spectra with the additional advantages mentioned above. Its implementation as a characterization tool in a synthetic laboratory, however, is not yet ubiquitous and as such has not been systematically applied to characterizing and studying cucurbit[*n*]urils.

Although Raman is immensely useful for characterizing bulk samples, it lacks the trace level sensitivity required for developing sensing applications using the molecular recognition properties of CB[*n*]s. However, the Raman signal can be enhanced 6 to 14 orders of magnitude with SERS allowing the spectral recognition of single molecules.[9,10] This is especially significant for chemical sensors operating in aqueous solution, where IR is overwhelmed by the signal from water. By appropriate patterning and optimization, metal plasmonic structures can be fabricated to give reproducible SERS enhancements.[11–15] Among these plasmonic substrates, Klarite™ is now commercially available.[16] SERS on reproducible surfaces is important for developing high throughput protocols, quantitative analysis and sensing applications.

We present for the first time a systematic study of cucurbit[*n*]urils using Raman spectroscopy. We also report for the first time SERS of CB[*n*]s while showing ppb (parts per billion) level detection capability and the ability to decipher mixtures. Thus, in this paper, we study CB[*n*] homologues with Raman and SERS spectroscopy and obtain systematic trends which provide evidence of the changes in the ring strain with increasing ring size. We assign the experimentally observed peaks by carrying out molecular simulations. Furthermore, we

[a] *Cavendish Laboratory, University of Cambridge, J. J. Thomson Avenue, Cambridge CB3 0HE, UK. E-mail: sm735@cam.ac.uk; Fax: +44 (0)1223764515; Tel: +44 (0)1223337050*
[b] *Melville Laboratory for Polymer Synthesis, Department of Chemistry, University of Cambridge, Lensfield Road, Cambridge CB2 1EW, UK. E-mail: oas23@cam.ac.uk; Tel: +44 (0)122331508*

† Electronic supplementary information (ESI) available: Peak frequencies for all CB[*n*], movies of vibrational modes, SERS spectra of individual CB[*n*] on Klarite, SERS with different CB[5] concentrations and size data (TEM) of CB[*n*]–gold nanoparticle conjugates. See DOI: 10.1039/c0cp00071j

demonstrate the utility of SERS for studying CB[*n*]s on a surface-enhancing substrate such as Klarite™ and its detection when conjugated directly to gold nanoparticles; paving the way for SERS-based sensitive molecular recognition and detection assays with the latter particularly promising for real-time monitoring of CB[*n*] supramolecular complexes in solution.

2. Experimental section

2.1 Materials

Gold(III) chloride trihydrate and sodium borohydride were purchased from Sigma Aldrich and Alfa Aesar, respectively, and were used as received.

2.2 Synthesis of cucurbit[*n*]urils and gold nanoparticle-capped cucurbit[*n*]urils

Synthesis of cucurbit[*n*]uril was carried out according to the reported procedure by Kim *et al.*[6] Isolation and purification were performed according to methods reported by our group.[17] Synthesis of gold nanoparticle-capped cucurbit[*n*]uril composites was done according to methods reported by our group.[18]

2.3 Raman/SERS

A Renishaw Raman InVia Microscope was employed. The Raman and SERS spectra on Klarite™ surfaces were acquired with a single scan of 10 s each using a 785 nm laser at 2.8 mW incident power on the sample. Klarite™ surfaces used in this work have a strong plasmonic resonance at 785 nm and hence are ideal for SERS measurements with the above laser. The SERS spectra on Klarite™ were recorded by placing 1 mM solution of the respective CB[*n*] in 20% DCl/D_2O and glass cover slip was placed on top. In DCl/D_2O all CB[*n*]s are soluble ensuring that the spectra are acquired under similar conditions. The SERS spectra for the conjugated nanoparticles were acquired with a 514 nm laser at an incident power of 1.1 mW with 3 accumulations of 30 s each. A 1200g grating was employed to give a spectral resolution of $\sim$4 cm^{-1}. For recording the SERS spectra a drop of 50 μl of $\sim$0.1 mM CB[*n*]–gold nanoparticle conjugate solution in aqueous ethanol was dried on a glass slide.

2.4 Simulations with Spartan '08

The starting geometry for CB[5], CB[6] and CB[8] was retrieved from the CSD database (cucurbit[5]uril tetrahydrate clathrate, refcode: LIRTEL, cucurbit[6]uril refcode: BEBDOP and cucurbit[8]uril refcode: REDMET) and subsequently geometry-optimized at Hartree–Fock (3-21G basis set) level of theory. For CB[7], the geometry was built invoking standard bond lengths and bond angles using Spartan Model Builder followed by step-wise geometry optimizations on PM3 and HF/3-21G. Upon geometry optimization D_{5h} symmetry was reached for CB[5] whereas CB[6]–CB[8] optimized structures were of C_{2h} symmetry. Vibrational modes and Raman intensities were calculated using Spartan's inbuilt algorithms whereby the symmetry option was disabled as D_{5h} symmetry for CB[5] has not been observed experimentally and thermal fluctuations are likely to cause distorted ground state geometries at ambient temperatures. A scaling factor of 0.90 was applied to correct the calculated vibrational frequencies as obtained with HF/3-21G for standard organic molecules.[19]

3. Results and discussion

Cucurbit[*n*]urils, where n = 5–8, were synthesized and purified according to published methods.[6,17] The dry powder of each CB[*n*] was subjected to Raman investigation. The Stokes-shifted Raman spectra of all the homologues are presented in Fig. 1. The finger-print region (400 cm^{-1} to 2000 cm^{-1}) in the Raman spectra shows clear and identifiable peaks for each CB[*n*]. The spectra compare well with the single Raman spectrum of CB[5] published by Corma *et al.*, in which neither the conditions nor any assignment have been reported.[20] Nevertheless, upon closer examination of the spectra of the homologues, it is seen that the peaks either increase or decrease in frequency with the number (n) of glycouril units of the CB[*n*]. In particular, the two most intense peaks in the spectra, at $\sim$830 cm^{-1} and $\sim$450 cm^{-1} blue and red shift, respectively, with an increase in ring size (Fig. 1b). The 450 cm^{-1} peak shifts negatively by 4 cm^{-1} and the 830 cm^{-1} peak shifts positively by 1–2 cm^{-1} per additional glycouril unit. The 883 cm^{-1} peak shifts much

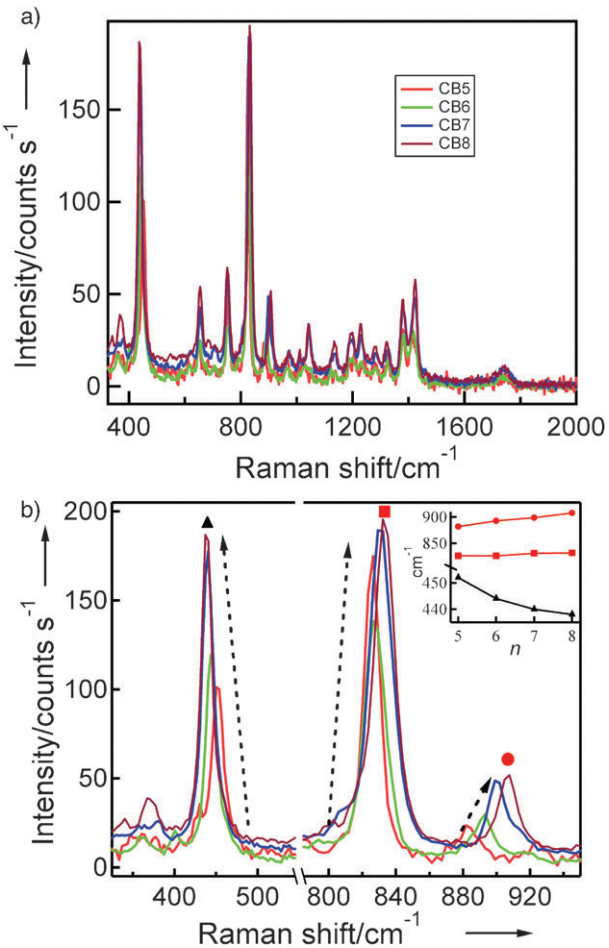

Fig. 1 (a) Raman spectra of CB[n = 5–8] in the 'fingerprint' region. (b) Peaks shift systematically with an increase in n. The variation of the marked peaks is shown in the inset. Acquisition conditions: 785 nm excitation, single 10 s scan.

more significantly by +8 cm^{-1} per additional glycouril unit. This amounts to a destabilization and stabilization, respectively, of −0.50 meV (450 cm^{-1}), +0.25 meV (830 cm^{-1}) and +1 meV (883 cm^{-1}). The other peaks seen in Fig. 1a do not shift significantly and hence have not been considered in the analysis below.

Computational simulation was carried out with Spartan '08 to visualize the Raman active vibrations in CB[n = 5–7] and compare frequencies with experimental results.[21] Qualitative correlation of peak positions could be obtained only when the symmetry of the molecule was disregarded in the calculations, pointing to the inherent asymmetry in the actual structure as confirmed in the reported X-ray crystal structures.[6] The peak assignments and frequencies for CB[5] and CB[7] are listed in Table 1 (see ESI† for all CB[n] peak assignments). The difference in the calculated and observed frequencies, even after correcting by a factor of 0.9 (usually employed in such HF calculations) is due to the small basis set (split-valence 3-21G) employed in the calculations.[19] HF/3-21G calculations on standard organic molecules are known to systematically overestimate bond strengths but reproduce the experimental trends and systematic changes for molecules with similar electronic environments. Nevertheless, the correlation with experimental results is good.

The 450 cm^{-1} is a 'ring' scissor mode (in-phase 'scissor' vibration along the N–C–N bonds of the 5-membered glycouril ring), the peak at 830 cm^{-1} is assigned to ring deformation modes (8-membered ring deforms out-of-phase with the 5-membered glycouril ring) while the 880 cm^{-1} is a complex ring breathing like mode (Fig. 2) comprising of deforming and twisting motions (see ESI† for movies of these vibrational modes). The simulations confirm the observations (Fig. 1) regarding peaks shifts with an increase in size of the cucurbit[n]urils studied here and this is discussed below.

Raman frequencies can be modelled using the harmonic oscillator ($\bar{\nu} \propto \sqrt{k/\mu}$) where the frequency will depend not only on the force constant (k) but also on the reduced mass (μ) of the atoms involved in the vibration. For cases involving the same atoms in different molecules, an increase in stretching frequencies can directly be inferred as an increase in bond stiffness. However, this simplistic analysis is not directly valid for deformations, scissors or twists present in macrocyclic ring structures such as cucubit[n]urils in which steric factors and bond angle strains can alter the overall stability/energy of the structure and therefore affect the vibrational frequency of a given mode.

Understanding these could be critical for deciphering differences in stability and reactivity of homologous cucurbiturils. Interestingly peaks (Table 1) associated with deformations, bends or twists increase or decrease in frequency with the CB[n] size. The simple stretches are mostly unaffected. This observation clearly implicates steric and ring strain factors for the observed systematic variation. The observed slight increase in frequency for the 830 cm^{-1} band with increasing size of the CB[n] is probably a result of increase in strain due to an increase in the regular sp^3 bond angle.

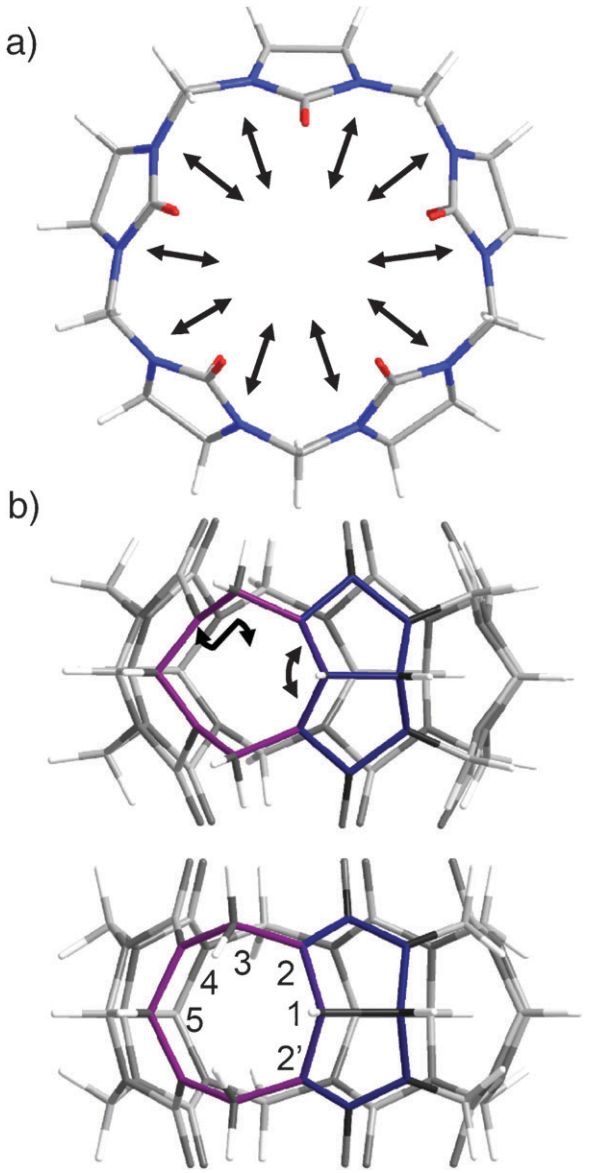

Fig. 2 Pictorial representation of CB[5] vibrations for the 881 cm^{-1} peak in (a) plan view depicting the overall ring breathing effect and in (b) side views showing the effect on the 8- and 5(glycouril)-membered ring as a result of the bending and twisting motions across N–C–N (2–1–2′) and N–C–C–N (2–3–4–5) bonds. The vibration snapshots have been obtained with Spartan '08.

Table 1 Raman frequencies and their assignments for CB[5] and CB[7]

CB[5]		CB[7]		
Observed	Calculated[a]	Observed	Calculated[a]	Assignment[a,b]
452	458	441	440	σN–C–N
655	644	655	646	τHC–CH
826	830	829	833	δC–N–C + ρCH_2
881	886	899	902	βC–N–C + τN–C–C–N + νC–C
1378	1360	1378	1361	Symmetric νC–N
1419	1417	1421	1420	Asymmetric νC–N
1745	1746	1745	1746	νC=O

[a] Based on Spartan '08 Hartree–Fock (3-21G) simulations. [b] ν = stretch, β = bend, δ = deformation, ρ = rock, σ = scissor and τ = twist.

However, for the 880 cm^{-1} vibration, additional repulsion between the N–CH–N and $–CH_2$ hydrogen atoms occurs, which are probably driven closer with an increase in the molecular size, resulting in a larger increase in frequency with an increase in macromolecular size. For the 450 cm^{-1} vibration the effect is opposite because it is a scissoring vibration involving the N–C–N bonds (the 5-membered glycoruril rings bend towards each other) and therefore becomes less strained with an increase in ring size.

Thus, Raman spectroscopy can be used for characterizing cucurbit[*n*]urils and identifying them in bulk samples. For trace level or surface based analysis, however, the SERS effect needs to be utilized. Here we employ the surface-enhancement of Klarite™ nanostructured surfaces to obtain SERS spectra of the CB[*n*] (see ESI†, Fig. S1). The trend in the shift of the 830 cm^{-1} and the 450 cm^{-1} peaks with increasing size (*n*) of the CB[*n*] is evident in the SERS spectra as well. We note that the SERS peaks are broader than their Raman counterparts, possibly due to weak interaction of molecular orbitals with the metal surface in the solution since CB[*n*] adsorbs on gold through interaction of their carbonyl groups with the metal surface.[22] With SERS detection it was possible to detect CB[5] even at the 10 ppb level in an aqueous solution. The SERS peak intensities were found to increase with concentration (see ESI†, Fig. S2). Furthermore, owing to the systematic shifts observed in the Raman peaks as a function of macromolecular size, the spectra remain distinguishable and allow for mixtures of CB[*n*]s to be analyzed. For example, CB[5] and CB[7] could be identified in a mixture of their aqueous solutions with SERS by deconvoluting the peak around 450 cm^{-1}. The spectra are presented in Fig. 3. It is pertinent to point out that during the synthesis of cucurbit[*n*]urils CB[5] and CB[7] are extracted as one fraction and CB[6] and CB[8] are separated as the second fraction, before further purification into individual components from their binary mixtures. Hence this result is significant as it presents a way of *in situ* analysis of the binary mixtures and monitoring the efficiency of purification procedure during the synthesis process. It is worth pointing out that the SERS analysis was done only with a single 10 s scan.

Gold nanoparticles can also act as SERS transducers in solution. We have recently synthesised cucurbit[*n*]urils capped by gold nanoparticles.[18] These nanoparticle conjugates present an attractive option for carrying out *in situ* SERS analysis directly in aqueous media. We present here preliminary data on the SERS of CB[n = 5–7] capped with gold nanoparticles in Fig. 4. The SERS spectra are obtained with a 514 nm laser tuned to excite the localized plasmons of gold nanoparticles causing the enhancement of the signals. Clear and unambiguous SERS peaks of CB[*n*]s conjugated to gold nanoparticles are seen. The inset in Fig. 4 shows the control spectrum of gold nanoparticles alone (without CB[*n*]s). Acquisition of *in situ* SERS spectra could prove immensely useful for deciphering binding mechanisms, real-time reaction monitoring and for developing applications in sensing with CB[*n*]s acting as selective hosts permitting the detection of analyte (guest) peaks. Further studies are under progress exploring these aspects and will be subject of a future publication.

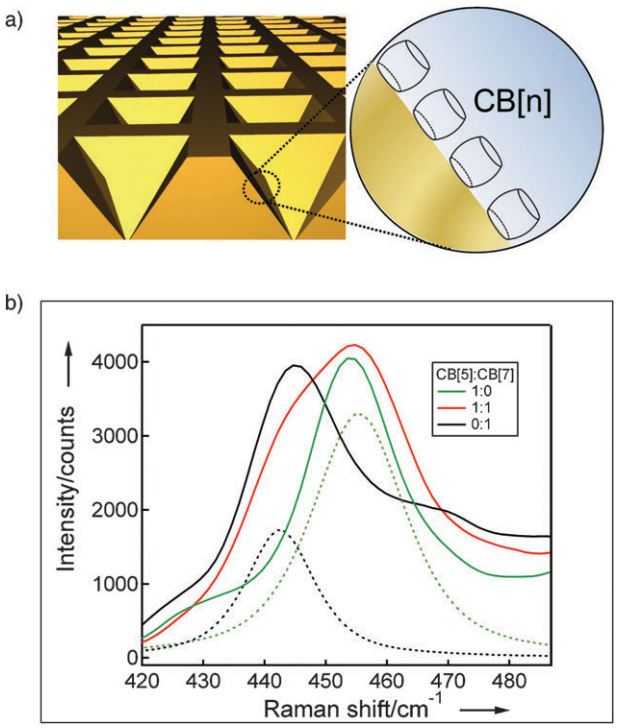

Fig. 3 (a) Schematic of CB[*n*] on Klarite™ nanostructured surface. (b) SERS spectra of 1 mM CB[*n*] solutions recorded on Klarite™. The deconvolved peaks (dotted) show the individual CB[5] and CB[7] components in the spectrum of the mixture. Acquisition conditions: 785 nm excitation, single 10 s scan.

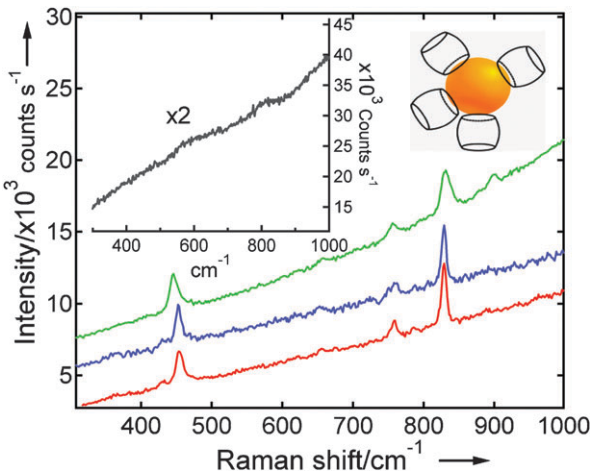

Fig. 4 SERS of CB[n = 5–7] conjugated to gold nanoparticles (CB[5] (red), CB[6] (blue), CB[7] (green)). The left inset is the control spectrum (×2) recorded on Au nanoparticles not conjugated to CB[*n*]s. Acquisition conditions: 514 nm excitation, 30 s scan, 3 accumulations. Spectra are offset for clarity.

4. Conclusions

In conclusion, we report for the first time a detailed study of all the major homologues of cucurbit[*n*]urils using Raman and SERS. Systematic shifts of the peaks are observed with increasing size of the CB[*n*]s. The observed trend is consistent in both Raman and SERS spectra. With the aid of computational

simulation, peaks have been assigned to their corresponding vibrational modes, providing a further rationalization of the observed spectra, as well as the shifts in vibrational frequencies. These shifts relate to changes in steric factors and bond angle strains with the size of CB[*n*]s which might help comprehend changes in their reactivity. Furthermore SERS has become an increasingly accurate and convenient way of characterization as well as identification at an ultra-sensitive level. Employing SERS we demonstrate characterization of CB[*n*]s, detection at an ultra-sensitive level of 10 ppb and differentiation in mixtures of CB[*n*]s, all of which will be highly advantageous in purification and isolation procedures as well in sensors. SERS of CB[*n*]s with conjugated gold nanoparticles opens up a host of new possibilities both aiding fundamental studies and sensing applications. Thus, this work not only establishes the use of Raman and SERS for the characterization and identification of CB[*n*]s but also is a significant step towards realizing ultra-sensitive molecular-recognition assays using SERS especially for aqueous chemical and supramolecular systems.

Acknowledgements

This work was supported by EPSRC EP/H007024/1 and EU NanoSci-E+ CUBiHOLE grants. F.B. thanks the German Academic Exchange Service (DAAD) for financial support.

Notes and references

1 J. Lagona, P. Mukhopadhyay, S. Chakrabarti and L. Isaacs, *Angew. Chem., Int. Ed.*, 2005, **44**, 4844.
2 M. V. Rekharsky, T. Mori, C. Yang, Y. H. Ko, N. Selvapalam, H. Kim, D. Sobransingh, A. E. Kaifer, S. Liu, L. Isaacs, W. Chen, S. Moghaddam, M. K. Gilson, K. Kim and Y. Inoue, *Proc. Natl. Acad. Sci. U. S. A.*, 2007, **104**, 20737–20742.
3 Y. Shen, S. Xue, Y. Zhao, Q. Zhu and Z. Tao, *Chin. Sci. Bull.*, 2003, **48**, 2694–2697.
4 W. L. Mock and N.-Y. Shih, *J. Org. Chem.*, 1983, **48**, 3618–3619.
5 M. D. Pluth and K. N. Raymond, *Chem. Soc. Rev.*, 2007, **36**, 161–171.
6 J. Kim, I.-S. Jung, S.-Y. Kim, E. Lee, J.-K. Kang, S. Sakamoto, K. Yamaguchi and K. Kim, *J. Am. Chem. Soc.*, 2000, **122**, 540–541.
7 S. Deroo, U. Rauwald, C. V. Robinson and O. A. Scherman, *Chem. Commun.*, 2009, 644–646.
8 C. Marquez, F. Huang and W. M. Nau, *IEEE Trans. Nanobiosci.*, 2004, **3**, 39–45.
9 K. Kneipp, Y. Wang, R. R. Dasari and M. S. Feld, *Appl. Spectrosc.*, 1995, **49**, 780–784.
10 S. Nie and S. R. Emory, *Science*, 1997, **275**, 1102–1106.
11 R. M. Cole, J. J. Baumberg, F. J. Garcia de Abajo, S. Mahajan, M. Abdelsalam and P. N. Bartlett, *Nano Lett.*, 2007, **7**, 2094–2100.
12 S. Mahajan, J. Baumberg, A. Russell and P. Bartlett, *Phys. Chem. Chem. Phys.*, 2007, **9**, 6016–6020.
13 S. Mahajan, R. Cole, B. Soares, S. Pelfrey, A. Russell, P. N. Bartlett and J. J. Baumberg, *J. Phys. Chem. C*, 2009, **113**, 9284–9289.
14 N. M. B. Perney, J. J. Baumberg, M. E. Zoorob, M. D. B. Charlton, S. Mahnkopf and C. M. Netti, *Opt. Express*, 2006, **14**, 847–857.
15 N. M. B. Perney, F. J. G. de Abajo, J. J. Baumberg, A. Tang, M. C. Netti, M. D. B. Charlton and M. E. Zoorob, *Phys. Rev. B: Condens. Matter Mater. Phys.*, 2007, **76**, 35426.
16 http://www.d3diagnostics.com.
17 D. Jiao, N. Zhao and O. A. Scherman, *Chem. Commun.*, 2010, **46**, 2007–2009.
18 T.-C. Lee and O. A. Scherman, *Chem. Commun.*, 2010, **46**, 2438–2440.
19 P. A. Scott and L. Radom, *J. Phys. Chem.*, 1996, **100**, 16502–16513.
20 A. Corma, H. Garcia and P. Montes-Navajas, *Tetrahedron Lett.*, 2007, **48**, 4613–4617.
21 Spartan 08 is available from Wavefunction, Inc., 18401 Von Karman Avenue, Suite 370, Irvine, CA 92612; www.wavefun.com.
22 Q. An, G. Li, C. Tao, Y. Li, Y. Wu and W. Zhang, *Chem. Commun.*, 2008, 1989–1991.